

## 6. Combination of the MRI-EPS and the MRI-AGCM3.2

### 6.1 MRI climate model (MRI-AGCM3.2)

Ensemble forecast experiments were performed by using a low-resolution version of the MRI-AGCM3.2 (Mizuta *et al.*, 2012). This model is based on the previous version of the JMA operational NWP model (GSM). Although several physical process schemes suitable for long-term integrations have been introduced into the model to facilitate its performance as a climate model, the fundamental part of the MRI-AGCM3.2 is common to the GSM, as described below. Results of long-term integrations with the MRI-AGCM3.2 have been verified from various points of view, and the model has been used for global warming research of the climate response to global warming conditions (e.g. Murakami *et al.*, 2011; Endo *et al.*, 2012). The model results are available for international use as one of the climate models in the Coupled Model Intercomparison Project Phase 5 (CMIP5; Taylor *et al.*, 2012). Furthermore, the model is used as the atmospheric component of the MRI-CGCM3 (Yukimoto *et al.*, 2011) and the earth system model MRI-ESM1 (Adachi *et al.*, 2013).

It is easy to configure experimental settings of the MRI-AGCM because it is developed for numerical experimental studies. Moreover, because the MRI-AGCM is a part of the earth system model, we can easily extend the experiments by coupling the other model components, such as the ozone chemical transport model.

The resolution of the model is set to be the same as that of the GSM used in the BGM cycle, which is TL159 (a grid interval of roughly 110 km) in the horizontal and 60 levels (top at 0.1 hPa) in the vertical. The dynamical framework is the same as that of the GSM, which is a hydrostatic primitive equation system that uses a spherical harmonic spectral transform method. The radiation scheme, the orographic gravity wave drag scheme, and the planetary boundary layer scheme are also the same as those in the GSM. Different physical process schemes are used for cumulus parameterization, cloud physics, land surface, and direct effects of aerosols. A new cumulus parameterization scheme has been developed, called the Yoshimura scheme (Yukimoto *et al.*, 2011; Yoshimura *et al.*, in preparation). The Tiedtke cloud scheme (Tiedtke, 1993) has been incorporated and is used in the model (Kawai, 2006). The model uses the land surface scheme of Hirai *et al.* (2007), which has been improved from the Simple Biosphere model (Sellers *et al.*, 1986) used in the GSM. More aerosol species are prescribed to calculate the direct effect of aerosols in detail. Details of the physical processes are described in Mizuta *et al.* (2012) and Yukimoto *et al.* (2011).

A normal-mode initialization scheme suitable for high-resolution global models (Murakami and Matsumura, 2007) has been applied to remove initial shock before integration of the MRI-AGCM3.2. The initial conditions for the land surface scheme are given by climatology with seasonal variation. The anomaly of the SST from the seasonally varying climatology is fixed

throughout the forecast experiments; the settings are the same as those used in the BGM cycle.

## 6.2 Temporal evolution of bred modes in various models

In this subsection, we examine the temporal evolution of the bred mode in the MRI-AGCM3.2. It should be noted that the BGM cycle generating the bred mode is based on the GSM, but not on the MRI-AGCM3.2. Because the adiabatic baroclinic instability process largely controls the temporal evolution of the bred mode, physical processes such as cumulus convection and radiation play only a secondary role. Hence, we can anticipate that the temporal evolution of bred modes is almost independent of the NWP model describing the evolution over time. Figure 11c compares the temporal variation of the amplification of each bred mode during the initial one-day temporal integration conducted by the MRI-AGCM3.2 (black lines) and by the GSM (red lines). This comparison confirms that the evolution over time is almost independent of the NWP model. We have therefore ascertained that the bred mode obtained with a BGM cycle based on the GSM is suitable for initial perturbations in ensemble forecast experiments based on the MRI-AGCM3.2.

## 6.3 Dependence of the temporal evolution of the bred mode on the analysis data

The bred mode obtained with the BGM cycle depends on the analysis field. As described in Section 3.1, we use the JRA-25/JCDAS analysis to compute the bred mode. It is thus natural to use the same analysis dataset (JRA-25/JCDA) to provide an unperturbed initial condition (control run) for the ensemble forecast experiment. However, there could be a demand for use of another reanalysis dataset, such as the European Centre of Medium-range Forecasting Reanalysis data (ERA-interim; Dee *et al.*, 2011) to conduct an ensemble forecast experiment. We therefore wished to confirm the consistency of the model by using different reanalysis datasets from JRA-25/JCDAS in advance. For this purpose, we compared the temporal evolution of the bred modes based on the JRA-25/JCDAS reanalysis and on the ERA-interim. Figure 12 compares the amplification of the bred modes during the first day of the ensemble forecasts based on each analysis during a period of 8 days from 10 to 17 December 2001. This comparison confirms that the amplification of the bred modes is almost independent of the analysis used in the ensemble forecast. It is thus ascertained that the ERA-interim reanalysis can also be used to provide an unperturbed initial condition for ensemble forecast experiments with initial perturbations represented by the bred mode of the BGM cycle. This fact also implies that the large-scale atmospheric state (especially in the troposphere), which controls the temporal evolution of the bred mode, is almost independent of the reanalysis datasets. In the following section, we examine the predictability of a SSW by using the ERA-interim reanalysis dataset for the unperturbed initial condition and the bred modes generated on the basis of the JRA-25/JCDAS dataset.

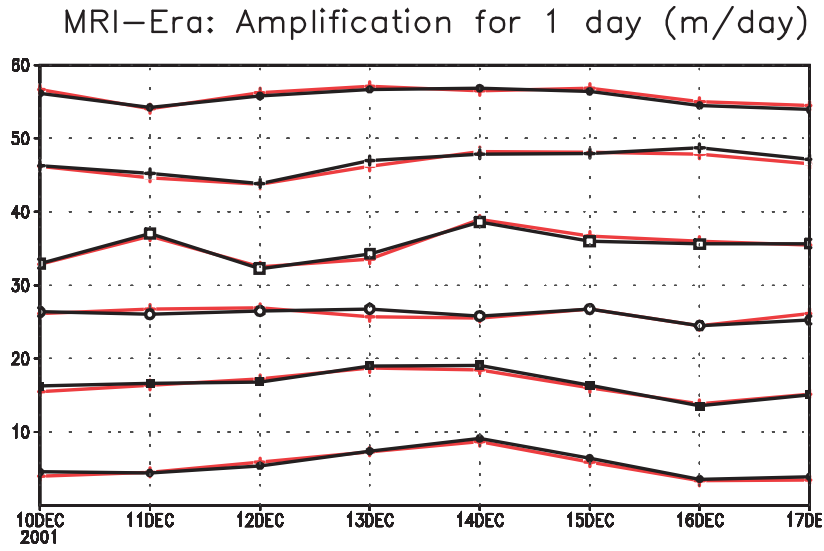


Figure 12: Same as in Figure 11c, except that the black lines indicate amplitude increments of bred modes obtained using the ERA-interim reanalysis data, and red lines for those obtained using the JRA-25/JCDAS reanalysis during the period from 10 Dec. to 17 Dec. 2001